Regions of stability in rotational dynamics

Alessandra Celletti, George Voyatzis

Celest Mech Dyn Astr (2010) 107:101–113
DOI 10.1007/s10569-010-9267-5

ORIGINAL ARTICLE

Regions of stability in rotational dynamics

Alessandra Celletti · George Voyatzis

Received: 6 November 2009 / Revised: 24 February 2010 / Accepted: 1 March 2010 /
Published online: 31 March 2010

Abstract We investigate the rotational dynamics of a triaxial planet moving on a Keplerian orbit around its star. The dynamics is ruled by several parameters, like the eccentricity, the obliquity, the non-principal rotation, the angular momentum, etc. We consider two specific cases in which the planet is symmetric or asymmetric, according to whether two moments of inertia coincide or differs from each other. We study the dynamics by constructing maps of dynamical stability based on the computation of the maximum Lyapunov characteristic number versus some typical parameters. The results show that only specific resonances appear in the symmetric case, while the asymmetric case shows a much richer phenomenology.

Keywords Rotational dynamics · Lyapunov exponents · Rotational resonances · Non-synchronous resonance · Stability maps · Triaxial planets

1 Introduction

The investigation of the rotational dynamics of the objects of the Solar System provides very interesting information about the stability and the internal structure of such bodies (see, e.g., Atobe and Ida 2007; Ferraz-Mello et al. 2008; Kitiashvili and Gusev 2008; Lemaitre et al. 2006; Noyelles 2008). Within rotational dynamics, a very special role is played by the so-called rotational resonances, which occur whenever the ratio of the period of revolution to the period of rotation is a rational number, say $p : q$ for some positive integers p and q. As it is well known, the Moon and the evolved satellites of the Solar System are trapped in a 1:1 (synchronous) resonance, while Mercury is observed to move in a 3:2 resonance around the Sun (Lemaitre et al. 2006; Dufey et al. 2009).

A. Celletti (✉)
Dipartimento di Matematica, Università di Roma Tor Vergata, 00133 Roma, Italy
e-mail: celletti@mat.uniroma2.it

G. Voyatzis
Department of Physics, Aristotle University of Thessaloniki, 54124 Thessaloniki, Greece
e-mail: voyatzis@auth.gr

In this work we want to address the question of how the selection of such resonances depends on the choice of the asymmetry parameter. More precisely, we consider a triaxial body (a planet) moving on a Keplerian orbit around its star with spherical mass distribution. We assume that the obliquity (namely, the angle formed by the direction of the angular momentum with the orbit normal) and the non-principal rotation angle (namely, the angle formed by the direction of the angular momentum with the planet's principal axis) are not zero. This model is ruled by some parameters, like the orbital eccentricity and the asymmetry parameter $(I_2 - I_1)/I_3$, where I_1, I_2, I_3 are the principal moments of inertia. The role of the eccentricity in the selection of the resonances has been already stressed (see, e.g., Celletti 1990a,b; Celletti and Chierchia 2008; Correia and Laskar 2004). Here we focus mainly on the difference of the dynamics between the cases of a symmetric ($I_1 = I_2 \neq I_3$) and an asymmetric ($I_1 \neq I_2 \neq I_3$) planet. The investigation of the dynamics is performed by computing the largest Lyapunov exponent versus some characteristic parameters, like the asymmetry parameter, the eccentricity or the angular momentum. Similar investigations have been performed in Pavlov and Maciejewski (2003), where the MEGNO indicator has been used to identify stable and unstable regions as a function of the parameters, and in Breiter et al. (2005), where MEGNO indicators and Lyapunov exponents have been computed to define stability maps for a particular case of the Kinoshita problem. The results found in the present paper are corroborated by the analysis of the coefficients of the Fourier series development of the potential, which correspond to the coefficients of the terms associated to the resonant normal form. Our study shows that in the symmetric case the only resonances that appear are of the type $p : 1$ for some positive integer p. Higher order resonances are present only when considering the asymmetric case. In that case there appear also resonances of the type $p : 2$ for some positive integer p. Moreover, the numerical investigation shows that the size of the chaotic region increases as the eccentricity gets larger as well as when the obliquity or the asymmetry parameter are bigger.

We have also studied the case of a planet composed by non-interacting core and mantle. The results show that also in this case the asymmetry of the planet plays an important role in the appearance of the $p : 2$ resonances, which are barely present in the symmetric case.

2 The rotational model

We consider a system composed by a rigid planet P with ellipsoidal shape, which moves on a fixed Keplerian orbit around a central star S. We denote by M the mass of the planet and by M_s the mass of the star. Let $I_1 < I_2 < I_3$ be the principal moments of inertia of the planet and let us introduce the quantities

$$C_2^0 \equiv \frac{I_1 + I_2 - 2I_3}{2}, \quad C_2^2 \equiv \frac{I_1 - I_2}{4}.$$

Denote by ℓ_0 the mean anomaly of the planet, by $\mathcal{G}$ the gravitational constant and by a the semimajor axis of the Keplerian orbit. We also denote by e the orbital eccentricity and by r, v the instantaneous orbital radius and the true anomaly. Both ℓ_0, r, v can be defined in terms of the eccentric anomaly u, and therefore of the time, by means of the following Keplerian relations:

$$\ell_0 = u - e\sin(u), \quad v = 2\arctan\left(\sqrt{\frac{1+e}{1-e}}\tan\left(\frac{u}{2}\right)\right), \quad r = a(1 - e\cos u).$$

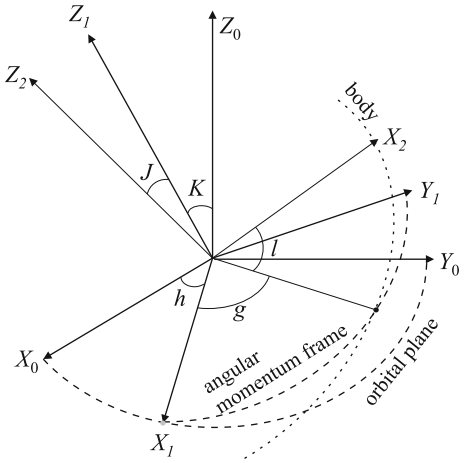

Fig. 1 The three reference systems with the non-principal rotation and the obliquity angles

In order to describe the rotation of the planet, we introduce three reference systems with origin at the barycenter of the planet (see Fig. 1):

- (X_0, Y_0, Z_0) denotes an inertial frame with the (X_0, Y_0)–plane coinciding with the orbital plane;
- (X_1, Y_1, Z_1) denotes the angular momentum frame with Z_1 oriented along the angular momentum direction;
- (X_2, Y_2, Z_2) is the body frame oriented along the principal axes of inertia.

The so-called Serret–Andoyer variables (G, L, H, g, ℓ, h) can be conveniently adopted to describe the rotational dynamics (Deprit 1967; Deprit and Elipe 1993). Their definition is the following: G denotes the angular momentum, $L = G\cos J$, $H = G\cos K$, where J, the non-principal rotation angle, is the angle between Z_1 and Z_2, while K, called the obliquity, is the angle between Z_1 and Z_0. The conjugated variables are defined as follows: g is the angle between X_1 and the line of nodes n_{mb} between the angular momentum and body frames; ℓ is the angle between the line of nodes n_{mb} and X_2; h is the angle between X_0 and X_1.

For the majority of the bodies of the Solar System the angles J and K are usually small; in that case it is convenient to introduce regular variables (Λ_j, λ_j), $j = 1, 2, 3$, which are defined as follows:

$$\begin{aligned} \Lambda_1 &= G & \lambda_1 &= \ell + g + h \\ \Lambda_2 &= G - L = G(1 - \cos J) & \lambda_2 &= -\ell \\ \Lambda_3 &= G - H = G(1 - \cos K) & \lambda_3 &= -h. \end{aligned} \tag{1}$$

In the following subsections we introduce different cases, according to the values of the principal moments of inertia, namely the symmetric case $I_1 = I_2$ or the asymmetric case $I_1 \neq I_2$.

2.1 Symmetric case $I_1 = I_2$

In the symmetric case $I_1 = I_2$, it turns out that $C_2^2 = 0$, so that the Hamiltonian reduces to the form (see, e.g., D'Hoedt and Lemaitre 2004; Lemaitre et al. 2006)

$$\mathcal{H}(\Lambda_1, \Lambda_2, \Lambda_3, \lambda_1, \lambda_2, \lambda_3, v) = \frac{\Lambda_1^2}{2I_1} + \frac{I_1 - I_3}{2I_1 I_3}(\Lambda_1 - \Lambda_2)^2 - \frac{\mathcal{G}M}{r^3}\left[\frac{C_2^0}{2}(2z^2 - x^2 - y^2)\right], \tag{2}$$

where (x, y, z) denote the components of the unit vector in the direction of the perturbing body, namely

$$\begin{pmatrix} x \\ y \\ z \end{pmatrix} = R_3(-\lambda_2)R_1(J)R_3(\lambda_1 + \lambda_2 + \lambda_3)R_1(K)R_3(-\lambda_3)\begin{pmatrix} \cos v \\ \sin v \\ 0 \end{pmatrix}.$$

We shall also write (2) in the form

$$\mathcal{H}(\Lambda_1, \Lambda_2, \Lambda_3, \lambda_1, \lambda_2, \lambda_3, v) = h_0(\Lambda_1, \Lambda_2) + V(\Lambda_1, \Lambda_2, \Lambda_3, \lambda_1, \lambda_2, \lambda_3, v),$$

where $h_0(\Lambda_1, \Lambda_2) \equiv \frac{\Lambda_1^2}{2I_1} + \frac{I_1 - I_3}{2I_1 I_3}(\Lambda_1 - \Lambda_2)^2$ and V is the potential. Going back to the original variables, the Hamiltonian takes the form

$$\mathcal{H}_1(G, L, H, g, \ell, h, v) = \frac{G^2}{2I_1} + \frac{I_1 - I_3}{2I_1 I_3}L^2 - \frac{\mathcal{G}M}{r^3}\left[\frac{C_2^0}{2}(2z^2 - x^2 - y^2)\right], \tag{3}$$

where the coordinates (x, y, z) are given by the transformation formulae:

$$\begin{pmatrix} x \\ y \\ z \end{pmatrix} = R_3(\ell)R_1(J)R_3(g)R_1(K)R_3(h)\begin{pmatrix} \cos v \\ \sin v \\ 0 \end{pmatrix}.$$

The coefficient C_2^0 is typically small and it can be considered as the perturbing parameter of the nearly-integrable system (3), whose integrable part depends only on G and L. Making the explicit computation of the potential, it can be easily seen that it does not depend on ℓ; therefore L is constant and the overall Hamiltonian depends only on G, H, g, h, v.

Next we provide the definition of rotational resonance. Let $\omega_{rev}, \omega_{rot}$ be, respectively, the revolutional and rotational frequencies of the planet. Let p, q be non-zero positive integers; a $p : q$ rotational resonance occurs whenever

$$\frac{\omega_{rot}}{\omega_{rev}} = \frac{p}{q}.$$

From (3) one gets that a $p : q$ rotational resonance is characterized by the following relation:

$$\dot{g} = \frac{G}{I_1} = \omega_{rot} = \frac{p}{q}\,\omega_{rev} = \frac{p}{q},$$

since ω_{rev} can be set to one by a suitable choice of the units of measure. Therefore one has

$$\dot{g} - \frac{p}{q} = 0,$$

so that the resonant angle corresponding to the order $p : q$ is given by the quantity $g - \frac{p}{q}t$.

In many astronomical cases the angle J is very close to zero and I_1 is approximately equal to I_2. The term appearing in the potential function can be written as

$$B \equiv 2z^2 - x^2 - y^2 = 3z^2 - (x^2 + y^2 + z^2) = 3z^2 - 1$$

and it turns out that $B = B(J, K, g, h, v)$, being

$$z^2 = \frac{1}{G^4}\Big(L\sqrt{G^2 - H^2}\sin(h - v) + \sqrt{G^2 - L^2}\Big(H\cos g \sin(h - v) + G \sin g \cos(h - v)\Big)\Big)^2.$$

The corresponding Hamiltonian takes the form

$$\mathcal{H}_1 = T + A(r)z^2,$$

where

$$T = \frac{G^2}{2I_1} + \frac{I_1 - I_3}{2I_1 I_3}L^2, \quad A(r) = -\gamma\frac{1}{r^3}, \tag{4}$$

having introduced the constant term $\gamma = \frac{3}{2}\mathcal{G}M\, C_2^0$. Since the Hamiltonian does not depend on ℓ, the action L is constant and the corresponding Hamiltonian depends just on (G, H, g, h, v). We now distinguish the cases of circular and elliptic motion.

If we assume circular motion, namely $e = 0$, then we have that the orbital radius is constant, say $r = r_0$, while the true anomaly reduces to the time, say $v = t$, once the mean motion has been normalized to one. As a consequence, the Hamiltonian becomes

$$\mathcal{H}_1 = T + \gamma'\frac{1}{G^4}\Big(L\sqrt{G^2 - H^2}\sin(h - t) + \sqrt{G^2 - L^2}\,(H\cos g \sin(h - t) + G \sin g \cos(h - t))\Big)^2, \tag{5}$$

where $\gamma' = \gamma/r_0^3$. From (5) it follows that the derivative $\dot{G}$ contains the multiplying factor $\sqrt{G^2 - L^2}$, so that the stationary solution $G = G_0$, being G_0 the initial condition, is obtained as far as $G = L$, which corresponds to the constraint $J = 0$. By using (4) we get that the kinetic part is constant and that the Hamiltonian reduces to

$$\mathcal{H}_1(H, h - t) = \tilde{\gamma}\sqrt{G^2 - H^2}\sin(h - t), \tag{6}$$

where $\tilde{\gamma} = \gamma' L/G^4$. By means of a trivial canonical transformation, one can reduce the Hamiltonian (6) to a one-dimensional autonomous case.
The solution $G = L$, namely $J = 0$, is also valid for an elliptic motion with non-zero eccentricity e. In this case the Hamiltonian (6) holds with

$$\tilde{\gamma} = \frac{\gamma L}{G^4}\frac{1}{r^3},$$

where the orbital radius depends on time. Therefore, the final Hamiltonian turns out to be one-dimensional with time-dependence and the equilibrium points of the autonomous system are replaced by periodic orbits.

2.2 Asymmetric case $I_1 \neq I_2$

If the moments of inertia are different from each other, the Hamiltonian can be written in the form

$$\mathcal{H} = \frac{L^2}{2I_3} + \frac{1}{2}(G^2 - L^2)\left(\frac{\sin^2 \ell}{I_1} + \frac{\cos^2 \ell}{I_2}\right) + V,$$

where the potential is given by

$$V = -\frac{\mathcal{G}M}{r^3}\left[\frac{C_2^0}{2}(2z^2 - x^2 - y^2) + 3C_2^2(x^2 - y^2)\right]. \tag{7}$$

Non-singular variables are defined as in (1); in terms of these coordinates, the Hamiltonian function is given by

$$\mathcal{H} = \frac{(\Lambda_1 - \Lambda_2)^2}{2I_3} + \frac{1}{2}(\Lambda_1^2 - (\Lambda_1 - \Lambda_2)^2)\left(\frac{\sin^2 \lambda_2}{I_1} + \frac{\cos^2 \lambda_2}{I_2}\right) + V,$$

with the potential V as in (7). When dealing with a $p : q$ rotational resonance, one can introduce the resonant angle

$$\sigma \equiv \lambda_1 - \frac{p}{q}\, t. \tag{8}$$

3 Resonances in symmetric and asymmetric cases

In order to investigate the different behaviors of the symmetric and asymmetric cases we perform a normal form analysis along the following lines. As already remarked, for $I_1 = I_2$ the term C_2^2 vanishes and the Hamiltonian becomes independent on the angle variable ℓ or, equivalently, on λ_2 (see Eq. 1) so that Λ_2 is constant. Introducing the resonant angle as in (8), with reference to (2) one obtains a Hamiltonian function of the form

$$\mathcal{H}(\Lambda_1, \Lambda_3, \tilde{T}, \sigma, \lambda_3, v; e, \Lambda_2) = h_0(\Lambda_1) - \frac{p}{q}\tilde{T} + V(\Lambda_1, \Lambda_3, \sigma, \lambda_3, v; e, \Lambda_2),$$

where $\tilde{T}$ is the variable conjugated to the time in the extended phase space. Notice that V depends on the small quantity C_2^0 and it depends parametrically on the orbital eccentricity e as well as on Λ_2. Let us expand the potential V in Taylor series of the eccentricity as

$$V = V_0 + eV_1 + e^2V_2 + \cdots .$$

Performing a standard first order perturbation theory, we can eliminate the dependence on the fast angle (the time). Let $\mathcal{C}_{p,q}^{20}(K, J)$ be the resonant coefficients associated to the resonant angle of order $p : q$; more precisely, the coefficient $\mathcal{C}_{p,q}^{20}(K, J)$ multiplies the term $\cos(2g - 2\frac{p}{q}t)$ in the development of the potential in Fourier series. We report below the

resonant coefficients associated to the main resonances:

$$\mathcal{C}^{20}_{1,1}(K,J) = -\frac{3}{4}\sin^2 J \left(1-\sin^2\frac{K}{2}\right)^2$$
$$\mathcal{C}^{20}_{3,2}(K,J) = -\frac{21}{8}e\ \sin^2 J \left(1-\sin^2\frac{K}{2}\right)^2$$
$$\mathcal{C}^{20}_{2,1}(K,J) = -\frac{51}{8}e^2\ \sin^2 J \left(1-\sin^2\frac{K}{2}\right)^2.$$

The above expressions of the resonant coefficients show that for small values of the eccentricity the 1:1 resonance dominates, since the 3:2 and 2:1 resonances are, respectively, of the first and second order in the eccentricity. Moreover, we remark that if J is small, the above coefficients become small.

A different situation occurs in the asymmetric case, in which there is also the contribution of the terms corresponding to C_2^2 as multiplying factors of the terms $\cos(2g - 2\frac{p}{q}t)$ in the Fourier development of the potential; in this case the resonant coefficients $\mathcal{C}^{22}_{p,q}(K,J)$ are provided below:

$$\mathcal{C}^{22}_{1,1}(K,J) = 3\left(1-\sin^2\frac{J}{2}\right)^2\left(1-\sin^2\frac{K}{2}\right)^2$$
$$\mathcal{C}^{22}_{3,2}(K,J) = \frac{21}{2}e\left(1-\sin^2\frac{J}{2}\right)^2\left(1-\sin^2\frac{K}{2}\right)^2$$
$$\mathcal{C}^{22}_{2,1}(K,J) = \frac{51}{2}e^2\left(1-\sin^2\frac{J}{2}\right)^2\left(1-\sin^2\frac{K}{2}\right)^2.$$

The analysis of the above coefficients shows that in the asymmetric case $I_1 \neq I_2$ the 1:1, 3:2, 2:1 resonances are not small if J is small, but their relative size depends on the value of the orbital eccentricity; for example, the terms of the 1:1 and 3:2 resonant coefficients become of the same order of magnitude as far as the eccentricity equals 0.28. The above expressions of the resonant coefficients provide the explicit expressions of the dependence of the resonances on the parameters J, K, e. This aspect will be further investigated through the computation of the dynamical stability maps as provided in the next section.

4 Dynamical stability maps

In order to explore the dynamics associated to the symmetric and asymmetric cases, we compute the maximum Lyapunov characteristic number for sets of initial conditions and parameters formed by fixing all parameters, except two of them. This allows us to obtain the so-called maps of *dynamical stability* (Celletti et al. 2007)[1] by drawing through a color scale the LCN values in the plane defined by the two variable parameters. We performed the numerical integrations for $t_{max} = 30000$ planetary revolutions. In Fig. 2 we present the LCNs of four trajectories showing different LCN values, including cases from a regular to a

[1] The maps of dynamical stability, also referred to as stability maps or dynamical maps, have been already computed in several works, like Erdi et al. (2004), Pavlov and Maciejewski (2003), Pilat-Lohinger et al. (2008), Voyatzis (2008), by using different chaos indicators. The color version of the maps is published in the online edition

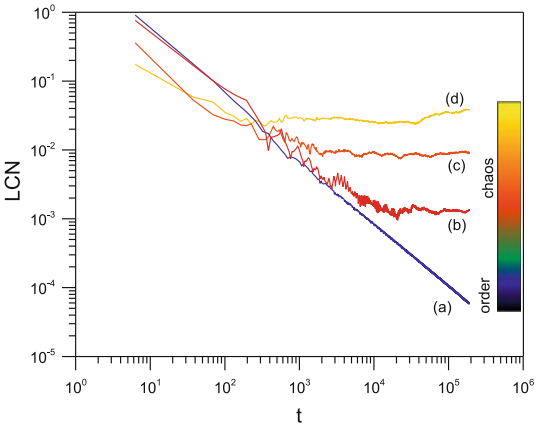

Fig. 2 The evolution of the LCN for four trajectories of the symmetric model with initial conditions: (*a*) $e = 0.4$, $\eta = 0.01$, $K = 1^\circ$ (regular), (*b*) $e = 0.01$, $\eta = 0.18$, $K = 1^\circ$ (weak chaos), (*c*) $e = 0.1$, $\eta = 0.1$, $K = 10^\circ$ (chaos), (*d*) $e = 0.1$, $\eta = 0.1$, $K = 30^\circ$ (strong chaos). For all cases $g = h = \ell = 0^\circ$, $G = 1$, $J = 1^\circ$. The color scale, which is used for the presentation of the LCN values in the stability maps, is shown

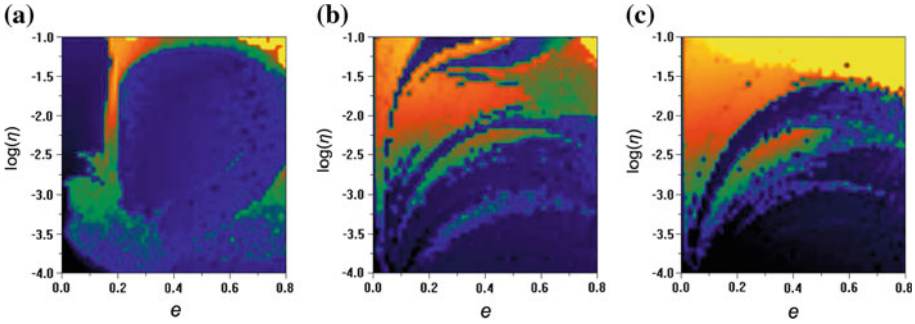

Fig. 3 Symmetric case $I_1 = I_2$; maps of dynamical stability for the initial conditions $G = 1$ (synchronous resonance), $J = 1^o$, $g = h = 0^o$. **a** $K = 1^o$, **b** $K = 10^o$, **c** $K = 30^o$ (See scale in Fig. 2)

strongly chaotic trajectory. In the stability maps, the final value of the LCN is displayed by using the color scale shown in Fig. 2.

In order to evaluate the dynamics as the asymmetry parameter $\eta \equiv (I_3 - I_1)/I_3$ and the eccentricity are varied, we report in Fig. 3 the dynamical stability maps obtained in the symmetric case for $G = 1$, which corresponds to the synchronous resonance, and for three different values of the obliquity K. The maps show that the chaotic regions become wider as the obliquity increases. However, when η is very small, we obtain regular trajectories for all eccentricities and even for large values of K.

To analyze the stability of the different resonances, we draw in Fig. 4 the maps in the plane $G - e$ for a given value of η and for three different values of the obliquity. The results show that the dominant frequency is the synchronous one, corresponding to $G = 1$ (for $e << 1$). Even for $G = 2$ a wide chaotic zone is apparent; other thinner chaotic zones exist as far as $G = 3$ and $G = 4$.

For the asymmetric case, we performed a set of LCN computations for different values of G and for some values of the planetary eccentricity. The results are shown in Fig. 5a. It is obvious that as the eccentricity increases, more and more intervals of G are associated with bigger LCN values indicating the enlargement of the chaotic regions. The computations

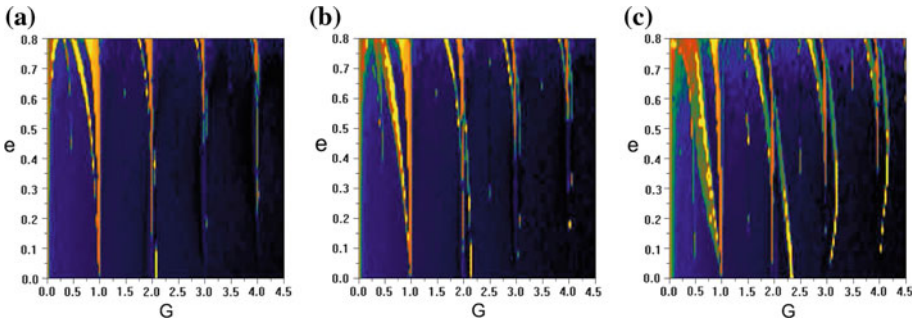

Fig. 4 Symmetric case $I_1 = I_2$; maps of dynamical stability for $\eta = 0.01$, $0 < G \leq 4.5$, $0 \leq e \leq 0.8$, and initial conditions $J = 1^{\circ}$, $g = h = 0^{\circ}$. **a** $K = 5^{\circ}$, **b** $K = 10^{\circ}$, **c** $K = 30^{\circ}$

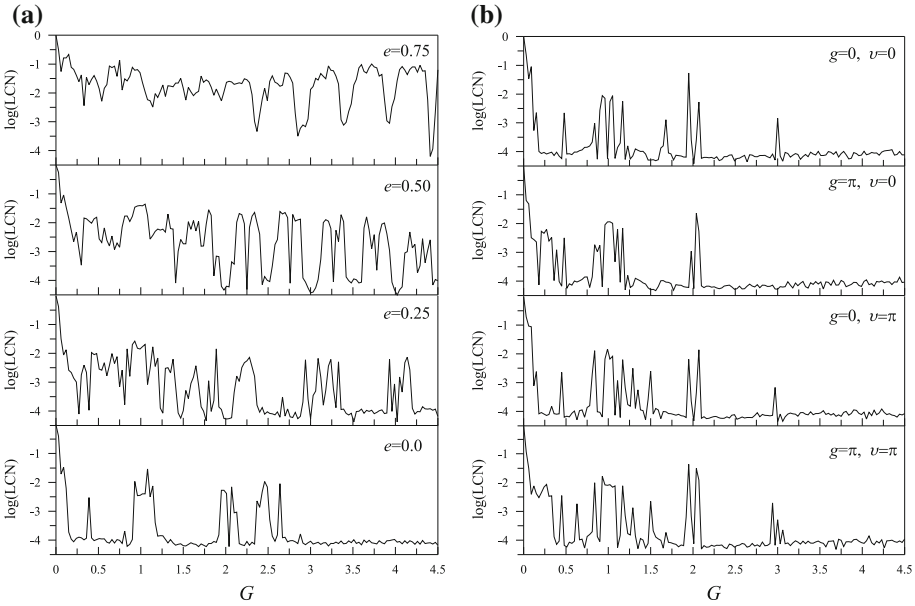

Fig. 5 Asymmetric case, $I_1 = 0.98$, $I_2 = 0.99$, $I_3 = 1$; graph of the Lyapunov characteristic number versus G with $0 < G \leq 4.5$. **a** $K = 25^{\circ}$, $J = 1^{\circ}$, $g = h = \ell = 0^{\circ}$, **b** $K = 5^{\circ}$, $J = 1^{\circ}$, $e = 0.1$, $h = \ell = 0^{\circ}$ and $(g, v) = (0, 0), (\pi, 0), (0, \pi), (\pi, \pi)$

presented were performed by considering the initial phase values $\ell = h = 0^{\circ}$. However, we observed that different values of initial angles in ℓ and h do not cause any significant difference. On the contrary, Fig. 5b shows how the dynamics is affected by the change of the fast angle phase g or of the true anomaly v, where $v = 0$ corresponds to the pericenter position and $v = \pi$ refers to the apocenter; for example, the 3:2 resonance at $G = 3/2$ becomes apparent for $v = \pi$.

A map of dynamical stability in the asymmetric case is provided in Fig. 6, which shows a striking difference with the symmetric case, since now all resonances are present through their separatrix chaotic layers, which surround the islands of regular librations associated to the resonant angle σ.

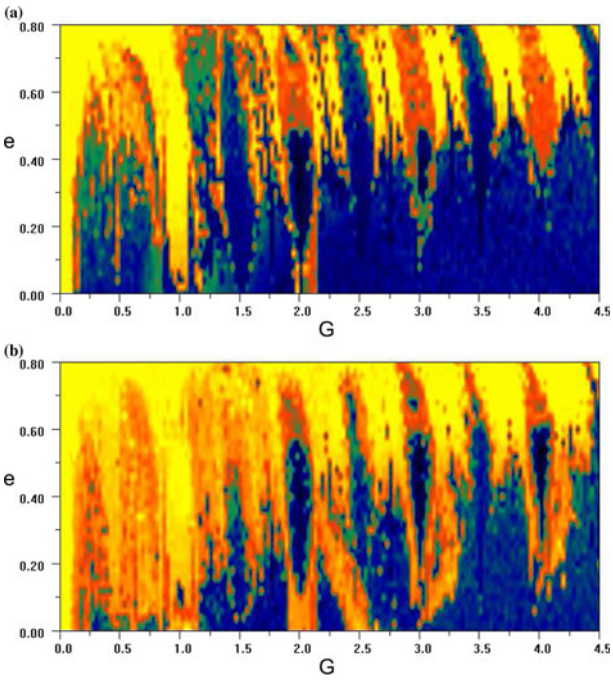

Fig. 6 Asymmetric case $I_1 = 0.98$, $I_2 = 0.99$, $I_3 = 1$; maps of dynamical stability for $0 < G \leq 4.5$, $0 \leq e \leq 0.8$, and for the initial conditions $J = 1^\circ$, $g = h = \ell = 0^\circ$, $e = 0.2$. **a** $K = 5^\circ$, **b** $K = 30^\circ$

Figure 7 shows the evolution of the resonant angle σ. In the asymmetric case (Fig. 7a) the resonant angle librates within the stability island around the resonance; the amplitude of libration increases when approaching the border of the island, while σ rotates outside in agreement with the classical resonant dynamics. In the symmetric case (Fig. 7b) slightly different initial conditions lead to a rotation of the angle, thus showing that we are not in a resonant regime.

5 Two layer problem

Assume that the planet is composed by two layers, a core and a mantle which are not interacting, and assume that the core has spherical shape. One can decompose the moments of inertia relative to the core (suffix c) and to the mantle (suffix m) as

$$I_1 = I_{1m} + I_{1c}, \quad I_2 = I_{2m} + I_{2c}, \quad I_3 = I_{3m} + I_{3c}, \tag{9}$$

where $I_{1c} = I_{2c} = I_{3c}$ due to the assumption of spherical core. The Hamiltonian of the two layer problem is given by

$$\mathcal{H} = \frac{L^2}{2I_{3m}} + \frac{1}{2}(G^2 - L^2)\left(\frac{\sin^2 \ell}{I_{1m}} + \frac{\cos^2 \ell}{I_{2m}}\right) + V,$$

where the potential V is given by (7) with the moments of inertia I_1, I_2, I_3 as in (9).

In order to draw the maps of dynamical stability, we need to assign specific values to the moments of inertia. Figure 8a provides the map (G, e) of dynamical stability centered

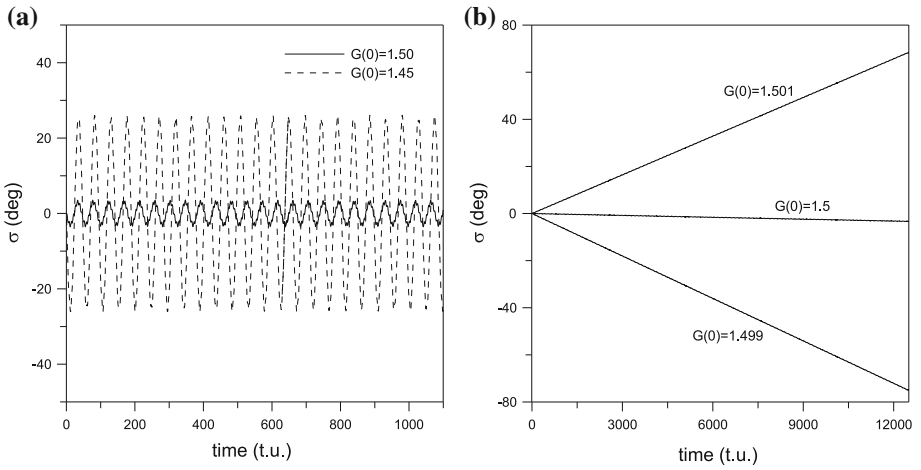

Fig. 7 The angle σ versus time in the **a** asymmetric and **b** symmetric case for three different initial values of G. The initial conditions are $K = 5°$, $J = 1°$, $g = h = l = v = 0°$; the parameters are $I_1 = 0.98$, $I_2 = 0.99$, $I_3 = 1$ for the asymmetric case, $I_1 = 0.99$, $I_2 = 0.99$, $I_3 = 1$ for the symmetric case

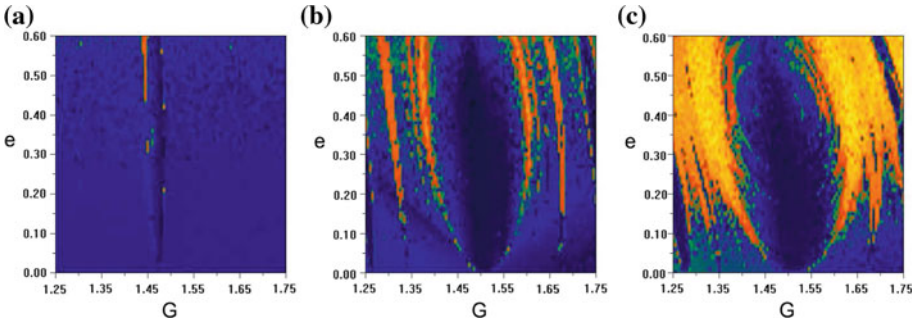

Fig. 8 **a** Two layer model with spherical core; maps of dynamical stability around the 3:2 resonance for $I_1 = I_2 = 0.99$, $I_3 = 1$, $K = 20°$, $J = 5°$, $g = h = \ell = 0°$. **b** Two layer asymmetric case; maps of dynamical stability around the 3:2 resonance for $K = 20°$, $J = 5°$, $g = h = \ell = 0°$, $I_1 = 0.99$, $I_2 = 0.995$, $I_3 = 1$. **c** Two layer asymmetric case; maps of dynamical stability around the 3:2 resonance for $K = 20°$, $J = 5°$, $g = h = \ell = 0°$, $I_1 = 0.98$, $I_2 = 0.99$, $I_3 = 1$

at $G = 3/2$ for a symmetric case in which we use the values $I_1 = I_2 = 0.99$ and $I_3 = 1$. Though the values of the obliquity and non-principal rotation angles are quite high to be realistic, the dynamics is almost everywhere regular and the 3:2 resonance is not really evident. Using asymmetric values as in Fig. 8b, c, the 3:2 resonance is definitely marked; the chaotic layer around the resonance increases as the asymmetry parameter $(I_2 - I_1)/I_3$ gets larger; this is displayed in Fig. 8b, c, where in panel (b) it is $(I_2 - I_1)/I_3 = 5 \cdot 10^{-3}$, while in panel (c) it is $(I_2 - I_1)/I_3 = 10^{-2}$.

6 Conclusions

The rotational dynamics has been investigated using two different settings, in which the rotating body is symmetric or asymmetric. These cases have been explored through the

computation of the maps of dynamical stability, providing the value of the Lyapunov exponent versus some parameters, like the eccentricity, the asymmetry parameter or the angular momentum G.

Our results show that the appearance of the resonances strongly depends on the choice of the asymmetry parameter. In particular, in the symmetric case there appear only resonances of order $p : q$ with $q = 1$, which dominate also for large values of the eccentricity. On the other hand, the dynamics is much richer in the asymmetric case, where many resonances appear. Wider chaotic regions are evident in this case and their extension increases as the eccentricity, the obliquity or the asymmetry parameter get larger. We note that a non-zero value of J implies that the model includes possible attitude instabilities (Wisdom et al. 1984). As J increases, chaotic regions get larger and significant changes in the dynamics can be expected.

We have also analyzed the case in which the rotating body is composed by two layers, namely a spherical core and a mantle, without assuming any interaction. We still find that resonances are much more marked in the asymmetric case with respect to the symmetric case. However, the 3/2 resonance is slightly more evident in comparison to the single layer model.

The development of further studies using more elaborated models will provide interesting information about the the link between the structure of the planet and its rotational dynamics. Such results are especially relevant in view of possible investigations of the rotational dynamics of exoplanets (compare with Atobe and Ida 2007; Ferraz-Mello et al. 2008; Kitiashvili and Gusev 2008), for which the observational data on the structure (i.e. moments of inertia) or rotational parameters (angular momentum, obliquity, etc.) are still very uncertain. However, it is worth stressing that many exoplanets are characterized by a large eccentricity comparable to those studied in this work, thus making possible a capture into a non-synchronous resonance.

Acknowledgments We thank Anne Lemaitre and Christoph Lhotka for useful discussions. A.C. acknowledges the ASI grant "Studi di Esplorazione del Sistema Solare" and PRIN 2007B3RBEY "Dynamical Systems and Applications" of MIUR.

References

Atobe, K., Ida, S.: Obliquity evolution of extrasolar terrestrial planets. Icarus **188**(1), 1–17 (2007)

Breiter, S., Melendo, B., Bartczak, P., Wytrzyszczak, I.: Synchronous motion in the Kinoshita problem. Application to satellites and binary asteroids. Astron. Astrophys. **437**, 753–764 (2005)

Celletti, A.: Analysis of resonances in the spin–orbit problem in celestial mechanics: the synchronous resonance (part I). J. Appl. Math. Phys. (ZAMP) **41**, 174–204 (1990a)

Celletti, A.: Higher order resonances and some numerical experiments (part II). J. Appl. Math. Phys. (ZAMP) **41**, 453–479 (1990b)

Celletti, A., Chierchia, L.: Measures of basins of attraction in spin–orbit dynamics. Celest. Mech. Dyn. Astron. **101**, 159–170 (2008)

Celletti, A., Kotoulas, T., Voyatzis, G., Hadjidemetriou, J.: A study of the dynamical stability in the Kuiper belt. MNRAS **378**(3), 1153–1164 (2007)

Correia, A.C.M., Laskar, J.: Mercury's capture into the 3/2 spin–orbit resonance as a result of its chaotic dynamics. Nature **429**, 848–850 (2004)

Deprit, A.: Free rotation of a rigid body studied in the phase plane. Am. J. Phys. **35**(5), 424–428 (1967)

Deprit, A., Elipe, A.: Complete reduction of the Euler–Poinsot problem. J. Astron. Sci. **41**(4), 603–628 (1993)

D'Hoedt, S., Lemaitre, A.: The spin–orbit resonant rotation of Mercury: a two degree of freedom Hamiltonian model. Celest. Mech. Dyn. Astron. **89**(3), 267–283 (2004)

Dufey, J., Noyelles, B., Rambaux, N., Lemaitre, A.: Latitudinal librations of Mercury with a fluid core. Icarus **203**, 1–12 (2009)

Erdi, B., Dvorak, R., Sandor, Z., Pilat-Lohinger, E., Funk, B.: The dynamical structure of the habitable zone in the HD38529, HD168443 and HD169830 systems. MNRAS **351**, 1043–1048 (2004)
Ferraz-Mello, S., Rodríguez, A., Hussmann, H.: Tidal friction in close-in satellites and exoplanets: the Darwin theory revised. Celest. Mech. Dyn. Astron. **101**, 171–201 (2008)
Kitiashvili, I.N., Gusev, A.: Rotational evolution of exoplanets under the action of gravitational and magnetic perturbations. Celest. Mech. Dyn. Astron. **100**, 121–140 (2008)
Lemaitre, A., D'Hoedt, S., Rambaux, N.: The 3:2 spin–orbit resonant motion of Mercury. Celest. Mech. Dyn. Astron. **95**, 213–224 (2006)
Noyelles, B.: Titans rotational state. Celest. Mech. Dyn. Astron. **101**(1–2), 13–30 (2008)
Pavlov, A.I., Maciejewski, A.J.: An efficient method for studying the stability and dynamics of the rotational motions of celestial bodies. Astron. Lett. **29**(8), 552–566 (2003)
Pilat-Lohinger, E., Suli, A., Robutel, P., Freistetter, F.: The influence of giant planets near MMR on Earth-like planets in the habitable zone of Sun-like stars. Astrophys. J. **681**, 1639–1645 (2008)
Voyatzis, G.: Chaos, order and periodic orbits in 3:1 resonant planetary dynamics. Astrophys. J. **675**, 802–816 (2008)
Wisdom, J., Peale, S.J., Mignard, F.: The chaotic rotation of Hyperion. Icarus **58**, 137–152 (1984)